AIAA Paper 97-2266, 15th AIAA Applied Aerodynamics Conference, June 23-25, 1997

Reduction of Narrow-Band Velocity Fluctuations Over an Aircraft Model

M. A. Klein† and N. M. Komerath§
School of Aerospace Engineering
Georgia Institute of Technology
Atlanta, GA 30332-0150

ABSTRACT

Surface fences are used to reduce the narrow-band velocity fluctuations observed over a 1/32-scale model of an F-15 at high angles of attack in a low speed wind tunnel. Previous work has traced these fluctuations to counter-rotating structures in the shear layer above the wing surface. A small vertical fence placed near the origin of the fluctuations attenuates the peak spectral energy by as much as 67% at 21.5° angle of attack. A narrow region is identified on the wing surface where fence placement attenuates the spectral peak, and fence size is optimized. A single fence location is identified where attenuation is achieved for angles of attack ranging from 16° to 34°. Comparisons with flight test accelerometer data confirm that the frequencies of significance to tail buffeting are the ones predicted in scaled model tests and attenuated by this technique. These results show that focusing on the surface shear layer, rather than on core instabilities, enables the engineer to take results obtained on small-scale wings and arrive at the optima found by trial and error on models with aeroelastic tails, and apply them to full-scale aircraft.

INTRODUCTION

This paper demonstrates the success of reducing twin-tail buffeting by using flow control on the wing surface of a fighter configuration. It then connects the results to what has been seen on larger elastically-scaled models and in full-scale flight tests. Surface fences are used to reduce the intensity of narrow-band velocity fluctuations in the vortical flow over aircraft with moderate wing sweep (<50 deg.) at high angles of attack (α). Previous work[1] has shown that such narrow-band fluctuations are common to models of existing combat aircraft, generic wing-bodies and to swept delta wings. The phenomena encountered on these configurations is different from the vortex core bursting which drives tail buffeting on the F/A-18 aircraft[2]. On the F/A-18, the vortex forming over a highly-swept (70-deg.) leading edge extension (LEX), has a strong core. At certain angles of attack, the core "bursts" over the wing, resulting in an increasingly chaotic flow enveloping the tail. The tail encounters large-amplitude fluctuations with a relatively broad spectral distribution, causing high levels of aerodynamic forcing.

When the wing sweep is below 50°, the vortex bursting phenomenon is generally not observed[3]. When α exceeds about 18°, the flowfield, beginning very near the wing-root juncture, appears to be a large swirling flow with no clear core. This has been declared to be a "post-burst" flow[4], but can be described more usefully as "never-unburst flow", due to the absence of any region where actual "bursting" occurs[5]. The key point is that there are no large-amplitude fluctuations to be seen: the broad-band spectrum of low-intensity fluctuations in an otherwise quasi-steady helical flowfield, has a low overall level of turbulence[6]. The difference is not merely semantic, as we show here, yet again: the "never-unburst" model has guided us to regions away from the center of the flow, and enabled systematic identification of other phenomena[7,8], which have in turn enabled elimination of the fluctuations[9]. In this paper, we extend those results to a scale model of an actual aircraft, the F-15, and tie our results on rigid-tailed 1/32-scale plastic hobby-shop models to past trial-and-error industry results on large scale models, with rigid and elastic tails, and to flight test results of the full aircraft. Success in tying all these observations together enables tail buffeting problems to be predicted and identified very early in the development of a new aircraft; as soon as the basic wing planform, tail geometry and tail placement can be determined, using results from small-scale models in low-speed tunnels. With passive or active flow control devices and some attention to the tail structural dynamic design, fatigue life of aircraft can be extended by eliminating the tuning between narrow-band flow fluctuations and elastic modes of the structure. Alternatively, the resources now expended on beefing up the tails can be made available for other things.

In contrast to the F/A-18 case, the fluctuations over the F-15 and other moderately-swept configurations start as a small blip in the velocity spectrum over the wing, in a region where the flow has no strong vortex core, and

†: USAF Senior Knight. Student Member, AIAA.
§: Professor. Associate Fellow, AIAA.

where the overall turbulence intensity is quite low. These fluctuations then amplify downstream and shift down in frequency. In front of the vertical tails, the spectrum of velocity fluctuations is sharply peaked, with much of the energy contained within a narrow frequency band. This is shown in Fig. 1, from Ref. 6. Starting from the "core breakdown" beliefs like most other researchers, we were faced with the question: *"why would a bursting core, degenerating into chaos, decide to re-organize itself downstream so that most of the fluctuation energy went into one narrow band, very nearly a single frequency?"* In Fig. 2, the scaled frequency of these fluctuations is constant over orders of magnitude of Reynolds number and extrapolates to the few data we had on large-scaled model and full scale flight test data[6].

We measured the helical trajectory of the fluctuations by tracking the coherence between two sensors[7,10], but this was not surprising, in view of the vortical mean flow pattern. The fluid mechanical origin of these fluctuations, and the mechanism of their amplification, remained in question. We reasoned that there are only a few flying aircraft configurations, so that empirical prediction was not an impractical approach. Our approach was two-pronged: basic experiments to find the phenomena, and empirical studies to develop empirical prediction and solutions. This paper reports the success of the latter, and its reinforcement of the results of the former.

Basic studies were continued on the 59.3° cropped delta wing, selected because it exhibited the vortex-bursting phenomenon,, and yet was of moderate-enough sweep to study the F-15-like phenomena. The flowfield was studied using hot-film probes[10], flow visualization[11], surface hot-film sensors and laser velocimetry[12] on a 59.3 deg. flat-plate delta wing, these fluctuations have been traced to counter-rotating structures, oriented along helical trajectories which lie nearly spanwise near the wing surface. These appear to be consistent with a centrifugal type of instability[8,9,12]. Using small fences, disruption of these structures near their origin has been shown to reduce the spectral peaks[9,12].

Demonstration of Attenuation on a Delta Wing

Ref. 13 summarizes previous work and the systematic examination of various hypotheses regarding the drivers of tail buffeting on moderately-swept aircraft configurations. Ref. 12 reports initial efforts to modify the fluctuation spectra by following the above observations of counter-rotating structures. As shown in Fig. 3, small fences were placed at various positions and orientations along a 59.3° delta wing surface to disrupt the generation of fluctuations at their origin, before amplification occurs. There is a region on the wing surface where up to 71% attenuation is achieved[9] The attenuation at the peak does not cause amplification at other frequencies, so a net attenuation of fluctuation energy is achieved. Hubner[12] mapped the contours of attenuation in a cross-flow plane at the wing trailing edge to ensure that the devices were not merely shifting the vortex flow pattern. Also, he showed the lift and drag characteristics were virtually unaffected by the fences. Ref. 9 proceeded to optimize fence location and height on the delta wing. Fig. 4 shows the effect of fence height on spectral peak attenuation[9]. Increasing fence height to about 6 mm on a 1/32-scale model gave increasing benefits; beyond this height, there was minimal additional reduction in the fluctuations. These data reinforce the evidence that the structures responsible for the narrow-band fluctuations originate near the wing surface, are not confined to the boundary layer and *do not originate in the core or central region of the vortex flow.* All three findings are consistent with the finding of spanwise-oriented, counter-rotating structures of the Görtler type. These are generated at the edge of the solid-body rotation region of the vortical flow above the wing surface, where there is a sharp radial gradient of tangential velocity. The fences, placed inboard of the secondary separation line apparently disrupt these structures just before they lift off the surface, preventing their further amplification before they arrive near the surface in the next turn of the helix.

Objectives

In this paper, we summarize the experience gained from the passive flow control experiments on the delta wing, and then apply this knowledge to an F-15 configuration. The most effective fence location is identified for the most critical α. The effectiveness of this fence is tested over the range of α where tail buffeting might be experienced. The F-15 is an aircraft on which some unclassified data are available, so that we can link our results on the systematic investigation of delta wings and several other aircraft configurations, to larger-scale industry tests, tests with elastic tails, and finally with flight tests. Success would provide confidence in using our techniques to anticipate and solve problems on future configurations, using inexpensive low-speed rigid scale model tests.

EXPERIMENTAL METHOD

Facility Description

The AeroControls Wind Tunnel at the School of Aerospace Engineering, is an open-return tunnel with the fan upstream of the 1.07 m x 1.07 m (42 in x 42 in) test section. Turbulence intensity is under 0.3%, and is mostly at the blade passage frequency. A single-sensor hot-film constant temperature anemometer probe was used to measure the velocity fluctuations, at various points in the flow. The sensor was placed perpendicular to the freestream direction (U_∞). The signal was digitized using a 16-bit, sample-and-hold analog-digital converter. One channel received the full hot-film signal, and a second channel received a band-pass filtered, amplified signal. The high and low pass were set at 0.1 Hz and 512 Hz. The gain was adjusted between 1 and 100 to optimize

precision. In each test, 50 sample blocks were used to calculate the ensemble averaged autospectrum. The resolution was 1 Hz and the Nyquist frequency was 256 Hz.

Model

The 1/32-scale F-15 model shown in Fig. 5 was assembled from a plastic hobby-shop kit, with steel plates strengthening the wings, tails and fuselage, and Bondo™ filling providing rigidity and mass. The engine inlets were sealed inside: the effects of flow-through and inlet droop on the spectra at the tails has been shown to be negligible[6]. The left vertical tail tip pod is removed so that a hot-film probe can take the place of the pod, with the sensor 25 mm upstream of the tail tip chord.

Test Cases

A baseline set of data was taken at the point in front of the tail by fixing α and varying velocity from 3.03 m/s (10 ft/s) to 21.4 m/s (70 ft/s). The α ranged from 16° to 36° in 2° increments. Fence lengths were then varied from 50.8 mm to 6.35 mm. Two fence heights were tested: 3.5 mm and 6 mm. To find the best fence height, length and location, U_∞ was fixed at 4.5 m/s α at 21.5°, of interest to the structural dynamics of the full-scale aircraft[14].

Fence locations are shown in Figs. 6 and 7; fences were used one at a time. The fences were placed with their leading edge at the identified position and aligned with the model center line. The locations are spaced in 10 mm or 20 mm increments with the first position being 20 mm downstream of the wing leading edge. Additional locations were used to refine the grid as needed. Once a fence height, length and location was identified for the best reduction of spectral peak intensity, its effectiveness was tested with increasing U_∞ and over a full range of α.

RESULTS

Fence Location

Our primary objective in this experiment was to apply the spectral peak reduction results from the 59.3° delta wing tests in Ref. 9 to an actual aircraft model, with its rounded leading edges, cambered, twisted wings, forebody, fuselage and inlets complicating the situation. For all the fences tested on the F-15 model, there is a region over the wing where attenuation is achieved. Unlike the 59.3° delta wing fence placement results, Fig. 6 shows only a small region where fences are effective in reducing spectral peak intensity. Out of this region, fences cause amplification; with significant amplification in close proximity to the maximum attenuation location. The fences used in Fig. 6 were very long in relation to the model scale; 25% of the semi-span. Shorter fences were tested to explore the small region of fence effectiveness.

Fig. 7 shows results for 6 mm x 25.4 mm fences in the narrow region near the wing leading edge and close to the wing/fuselage junction. Again, the locations shown in the figure identify the forward-most part of the fences. Fences placed between 0 and 20 mm outboard of the wing/fuselage junction and up to 40 mm downstream of the wing leading edge, measured at the particular outboard location, attenuate the fluctuations in the tail flowfield. These fences show up to 67% attenuation for α=21.5°. Fig. 8 shows examples of the spectral attenuation at α of 20° and 28°. At 50 mm downstream of the leading edge, amplification is seen. Due to the close proximity of maximum attenuation and amplification locations, the 10 mm outboard and 30 mm downstream fence position was chosen for further tests varying freestream and α. This position is referred to as fence location A in subsequent tests.

Spectral Attenuation

For angles of attack of 20° and 28°, Fig. 8 shows the F-15 velocity spectra for the with- and without-fence cases at freestream velocity U_∞=4.57 m/s. The 6 mm x 25.4 mm fences in the figure were at fence location A. Spectral attenuation is seen over the entire frequency range, with a 69% reduction at the spectral peak. The results for α=20° are representative of spectra found at $18° \le \alpha \le 22°$. Fig. 9 shows the peak spectral intensity reductions as a function of α. With the dramatic exceptions of 24° and 26°, there is a linear decrease in fence effectiveness with α from 18° to 34°. At 24°, fences are only 7% effective in reducing the intensity of the spectral peak. Effectiveness recovers somewhat at 26°, but not to the level of the linear trend seen at the other angles. At 24° and greater, there is an overall rise in broad-band spectra and a reduced fence effectiveness at frequencies away from the peak. An example of this is seen in the α=28° spectra in Fig. 8. Additional fence placement tests for α=24° showed no further reductions.

Fence Geometry Effects

It has been shown that a 6 mm x 25.4 mm fence at location A is effective through the entire α range. Further tests were run to determine if this fence configuration was effective as velocity was increased. Fig. 10 shows peak intensity variation with velocity for the with- and without-fence cases with the model at 21.5° α. Data in this figure are for fence location 6 which is 10 mm further downstream from location A. Percent reduction in the spectral peak is seen to slightly decrease with increase in velocity. This is primarily thought to be due to the widening of the spectral peaks as velocity is increased. This widening is caused by the flow fluctuations becoming less periodic. Again, the fences are seen to be most effective on reducing the periodic component of the flowfield. Once the fence location was defined, our objective was to minimize the fence length and height and identify an optimal orientation. By reducing fence size, any adverse effects on performance would also be minimized. It was seen in Fig. 4 for the 59.3° delta wing tests that fence heights above 6 mm showed little

additional effectiveness. Also, below 1 mm no effect was seen. Because of this, only two fence heights were tested; 3.5 mm and 6 mm. With fences at location A, Table 1 summarizes the fence size effects for α=21.5° and U_∞=4.57 m/s. Comparing the two 3.5 mm high fences, a 50.8 mm and a 12.7 mm long fence produce the same level of attenuation. Increasing the fence height from 3.5 mm to 6 mm for the 12.7 mm long fences increases the spectral peak intensity reduction from 32% to 43%. Doubling the length of the 6 mm x 12.7 mm fence to 6 mm x 25.4 mm produces a 64% attenuation. Halving the length of the 6 mm x 12.7 mm fence to 6 mm x 6.3 mm produces 17% attenuation. It is interesting to note that such a small fence placed in a seemingly chaotic flowfield can have a large effect on the development of nearly periodic fluctuations near the tails. The 6 mm x 25.4 mm fences were selected as the 'best' fence size.

Table 1 Spectral peak reductions with various fence sizes on F-15 model.

Fence size	Percent reduction
3.5 mm x 50.8 mm	32%
3.5 mm x 12.7 mm	32%
6 mm x 12.7 mm	43%
6 mm x 25.4 mm	64%
6 mm x 6.3 mm	17%
Note: Fence location A,	α=21.5°, U_∞=4.57 m/s

Further tests were performed to determine the effect of fence orientation relative to the model centerline on attenuation. Table 2 summarizes the orientations tested. In this table, positive fence angle is defined with the fence leading edge at fence location A and the fence trailing edge at the given angle inward towards the model centerline. Thus, a -45° fence angle is parallel with the wing leading edge. In general, both positive and negative orientations produced reductions in fence effectiveness. Only at +15° orientation was a greater reduction seen; a 1% greater reduction. No real benefit is seen over the model centerline oriented fences, and this orientation is also preferred due to concerns about low α drag, if the fence is mounted as a permanent fixture on the wing, rather than being deployed at high α.

Table 2 Spectral peak reductions with various fence orientations on F-15 model.

Fence Angle	Percent reduction
-45°	30%
-30°	57%
-15°	54%
0°	64%
15°	65%
30°	59%
45°	46%
Note: 6 mm x 25.4 mm, fence location A.	α=21.5°, U_∞=4.57m/s,

Spectral Characteristics

As mentioned previously, Fig. 9 shows a dramatic decrease in fence effectiveness at α of 24°. The marked change in fence effectiveness is attributed to the marked change in the velocity spectra characteristics at 22° < α < 28°. First, in this angle range, Fig. 11 shows an order of magnitude jump in peak spectral intensity, with a maximum between 26° and 28°. Where at lower α's a spectral peak dominates the broad-band spectra, this is not the case for α=24° and 26°. Fig. 12 shows the broad-band turbulent spectra at 24° has risen to a point such that the spectral peak in almost unrecognizable. A peak frequency versus velocity plot of the data for this angle remains linear, thus showing the nearly periodic fluctuating nature of the flow is still present. The broad-band spectra has become the dominant characteristic of the flow at this α. At higher angles, the spectral peak dominance reemerges and the fences regain their effectiveness on reducing the peaks, but the fence effectiveness on reducing the broad-band spectra is lost; as seen in Fig. 8. Again from Fig. 9, the fence percent reduction effectiveness is seen to decrease nearly linearly with α, with the exception of this 22°< α < 28° range.

From Colvin, et. al.[14], Fig. 13 shows full scale and 13% scale F-15 tail accelerometer data. Tail response is seen to dramatically increase where sharp narrow-band spectra are present at the tails; even when the magnitude is small (α<22°). When there is the order of magnitude of increase in overall turbulence level, and there is no dominant spectral peak, (i.e., 24°< α < 26°), the tail response is seen to rapidly decrease. At α>28° when the spectral peak becomes somewhat dominant again and the spectral intensities show a decrease, the tail response begins to level off and decrease in intensity less rapidly. Thus, F-15 tail buffet is shown to be driven by the small amplitude, narrow-band fluctuation at the tail and not by intense broad-band turbulence. It is precisely this narrow-band fluctuation that we are destroying with the fences. We are not "redirecting" the flow, or cutting off the spanwise flow: if these had been the case, the broad-band turbulence portion should also have been affected. Instead, the fences are serving to prevent amplification of the well-organized counter-rotating structures, just before they leave the surface shear layer where they are formed.

DISCUSSION

F-15 tail buffet has been a concern for more than 25 years[14-17], but no clear mechanism had been identified as responsible for the generation of flowfield fluctuations. The F/A-18, on the other hand, has been the catalyst for the research on highly-swept delta wings where vortex breakdown and other instability mechanisms have been identified. Refs. (18-25) are a tiny subset of what has been published on the F/A-18 and similar problems. The traditional approach to tail fatigue problems has been to stiffen the structure, under the assumption that the structure is excited by intense broad-band turbulent

fluctuations. Ashley, et al[17] have proposed active control of the F-15 rudders using tail-mounted actuators to cancel out the buffeting. Reductions in F/A-18 buffet response were reported by Roa. Puram and Shan[24] with modifications of the leading edge extensions, but lift performance was adversely effected. A recent F/A-18 design modification places small fences outboard on the F/A-18 LEX, upstream of the wing junction. Full scale wind tunnel tests on the F/A-18 by Meyn and James[25] have shown reductions of the peak power for angles of attack less than 40° and attenuation of the magnitude of the maximum peak power by nearly 50%.

Comparison with Aeroelastic Tests

Regardless of the success demonstrated in small-scale model tests at low speed, the questions remain whether (a) the same modifications would work at larger scales, and (b) whether the suppressed fluctuation is indeed relevant to tail buffeting on the full-scale aircraft. The final link in this puzzle comes by comparison with wind tunnel tests performed in 1979-82 by the McDonnell Aircraft Company (MCAIR) in their "F-15 vertical tail dynamic reduction program." The only documentation we have found on these experiments comes from a MCAIR presentation given in Ref. 16. The tests were performed on a 13% model with a flutter model empennage, where tail accelerometer data was used to determine changes in tail response. Fig. 6 shows the MCAIR optimized fence location for attenuation of buffet response at 22° α. Translated to our 1/32-scale model, the location on the 1/32-scale F-15 is 5 mm outboard of the wing/fuselage junction and 60 mm down from the leading edge. The fence size was then optimized at this location; which is 47.8 mm x 6.75 mm on the 1/32-scaled model. At a dynamic pressure of 12 PSF, a 30% reduction in tip pod acceleration was achieved. Although we have data for locations and lengths of fences very near the MCAIR optimum fence location, our fence height was only 3.5 mm. Our nearest data point showed a 58% amplification with a 3.5 mm x 50.8 mm fence. We have shown that fence height has a large effect on peak reductions, so the MCAIR reductions with a higher fence at this location are reasonable based on our data. Fences on the F-15 are reported to have a "fatigue life improvement factor" of 2, where the minimum desired was 10. This appears to be why fences were not pursued further. Perhaps this finding should be re-examined in the light of the observations made above. To close the issue of relevance, note that the last data point in Fig. 2 is from the spectrum of tail vibrations measured by the tip pod accelerometer in full-scale flight test at Mach 0.6.

Results on a simplified delta wing configuration identifying the source of the fluctuations and a method of attenuation have been shown to apply to an actual aircraft configuration. We note that everything seen to-date supports our hypothesis[13,8] of centrifugal instability generating counter-rotating structures in the shear layer above the wing surface, inboard of secondary separation. The phenomenon persists over orders of magnitude in Reynolds number and velocity, and is insensitive to the details of leading edge shape, as might be expected. It is seen both when there is a strong core breaking down upstream, as in the case of a 59.3° delta wing, and when there is not, as over an F-15 at $\alpha > 20°$. This success provides further support to our centrifugal instability hypothesis as the most basic phenomenon driving tail buffeting at high angles of attack.

CONCLUSIONS

The following conclusions are made:

1. The peak of the velocity spectrum upstream of the vertical tail is attenuated at every α on a 1/32-scale F-15 model by a fence placed at the optimum location to suppress fluctuations at $\alpha = 21.5°$. For $\alpha < 24°$ the intensity over the entire frequency range is reduced, with the peaks being reduced by more than 60%. For $\alpha > 24°$ broad-band fluctuations appear, so that there is only, a 20% to 40% reduction in the peak intensity. There is only an 7% reduction in the spectral peak at 24° when measured in terms of the total spectral level in the frequency interval.
2. There is only a small region on the F-15 wing where fences show effectiveness in reducing spectral intensity: near the wing leading edge and slightly outboard of the wing/fuselage junction.
3. Even 6 mm x 6.3 mm fences at location A reduce peak spectral intensity by 17%.
4. Fences at a single location remain effective with increase in freestream velocity and with increase in α.
5. Energy associated with the spectral peak is not shifted to another frequency band.
6. Further reductions in overall spectral level at $\alpha=24°$ may not be feasible due to the broad-band turbulent flowfield at this one angle.
7. F-15 tail buffet is shown to be driven by the small amplitude, narrow-band fluctuating nature at the tail and not by intense broad-band turbulence. It is precisely this narrow-band fluctuation that the fence suppresses.
8. The results of optimization from our 1/32-scale rigid model experiments correspond closely to those obtained by the manufacturers of the aircraft in wind tunnel tests of a large elastic model. Our optimization was guided by experiments on a generic delta wing.
9. The flight test accelerometer data confirm that the condition of maximum tail buffeting matches the condition where the velocity spectrum has the sharpest narrow-band peak: the frequency matches our prediction for that velocity and α, and this is also where the fence works best.
10. Empirically-based prediction and avoidance of twin-tail buffeting appears to be feasible, given the external geometry of the wings and tail placement. Wing leading edge shape, fuselage and inlets are secondary factors in this prediction.

ACKNOWLEDGMENTS

The first author is supported by the Air Force Palace Knight program. Assistance from the team members of the GT Experimental Aerodynamics Group (GTEAG) is gratefully acknowledged.

REFERENCES

1. Klein, M.A., Hubner, J.P., Komerath, N.M., "Spectral Measurements in Vortex Flow over Swept-Winged Configurations at High Angle of Attack". AIAA 94-1804, June 1994.
2. Wentz, W. H., Jr. and Kohlman, D. L., "Vortex-Fin Interaction of a Fighter Aircraft," AIAA 87-2474, 1987.
3. Lowson, M. V. and Riley, A. J., "Vortex Breakdown Control by Delta Wing Geometry," *Journal of Aircraft*, Vol. 32, No. 4, Jul-Aug, 1995.
4. Gursul, I., "Unsteady Flow Phenomena Over Delta Wings at High Angle of Attack," *AIAA Journal*, Vol. 32, No. 2, Feb. 1994, pp. 225-231.
5. Komerath, N.M., Liou, S-G., Schwartz, R.J., Kim, J-M., "The Flowfield of a Twin-Tailed Aircraft at Angle of Attack. Part I: Spatial Characteristics". *J. Aircraft*, 29, 3, May-June 1992, pp. 413- 420.
6. Komerath, N. M., Schwartz, R. J., and Kim, J. M., "Flow over a Twin-Tailed Aircraft at Angle-of-Attack, Part II: Temporal Characteristics," *Journal of Aircraft*, Vol. 29, 4, 1992, pp. 553-558.
7. Hubner, J.P. and Komerath, N.M., "Spectral Mapping of Quasiperiodic Structures in a Vortex Flow." *Journal of Aircraft*, Vol. 32, 3, May-June 1995, pp. 493-500.
8. Hubner, J.P. and Komerath, N.M., "Counter-Rotating Structures Over a Delta Wing". *AIAA Journal*, Vol. 34, No. 9, September 1996, pp. 1958-1960.
9. Klein, M.A., Lentz, W.K. and Komerath, N.M., "Reduction of Fluctuations over Swept Wings Using Passive and Active Mini-Fences," AIAA 97-0548, Jan. 1997.
10. Hubner, J.P. and Komerath, N.M., "Coherence-tracking of quasi-periodic structures in a vortex flow." AIAA 93-2914, July 1993.
11. Hubner, J. P. and Komerath, N. M., "Visualization of Quasi-Periodic Structures in a Vortex Flow," AIAA 94-0624, Jan. 1994.
12. Hubner, J. P. and Komerath, N.M., "Modification of Spectral Characteristics in a Vortex Flow Field," AIAA 95-1795, June 1995.
13. Komerath, N.M., "Development of Narrow-Band Velocity Fluctuations in Vortex Flows". AIAA 95-2304, June 1995.
14. Colvin, B. J., Mullans, R. E., Paul, R. J., and Roos, H. N., "F-15 Vertical Tail Vibration Investigations," MDC Report A6114, McDonnell Aircraft Co., St. Louis, MO, Sept. 1979.
15. Triplett, W. E., "Pressure Measurements on Twin Vertical Tails in Buffeting Flow," *Journal of Aircraft*, Vol. 20, No. 11, 1983, pp. 920-925.
16. Colvin, B. J., "F-15 Vertical Stabilizer History," McDonnell Aircraft Company, presentation at advisory committee meeting to develop new F-15 vertical stabilizer design criteria, 28 Nov. 1988.
17. Ashley,.H., Rock, S. M., Chaney, K. and Eggers, Jr., A.J., "Active Control fro Fin Buffet Alleviation," WPAFB, WL-TR-93-3099, 1993.
18. Gad-el-Hak, M., and Blackwelder, R. F., "Control of Discrete Vortices from a Delta Wing", *AIAA Journal*, Vol. 25, No. 8, 1987, pp. 1042-1049.
19. Payne, F. M., Ng, T. T., Nelson, R. C., and Schiff, L. B., "Visualization and Wake Survey of Vortical Flow over a Delta Wing," *AIAA Journal*, Vol. 26, No. 2, 1988, pp. 137-143.
20. Lowson, M. V., "Visualization Measurements of Vortex Flows," AIAA 89-0191, Jan. 1989.
21. Reynolds, G. and Abtahi, A., "Three-Dimensional Vortex Development, Breakdown, and Control," AIAA 89-0998, Mar. 1989.
22. Rao, D. M., Puram, C. K. and Shan, G. H., "Vortex Control for Tail Buffet Alleviation on a Twin-Tail Fighter Configuration," SAE 892221, Sept. 1989.
23. Lee, B. H. K., and Brown, D., "Wind Tunnel Studies of F/A-18 Tail Buffet," *Journal of Aircraft*, Vol. 29, No. 1, 1992, pp. 146-152.
24. Washburn, A. E., Jenkins, L. N., and Ferman, M. A., "Experimental Investigation of Vortex-Fin Interaction," AIAA 93-0050, Jan. 1993.
25. Meyn, L. A., and James, K. D., "Full-Scale Wind Tunnel Studies of F/A-18 Tail Buffet," AIAA 93-3519, Aug. 1993.

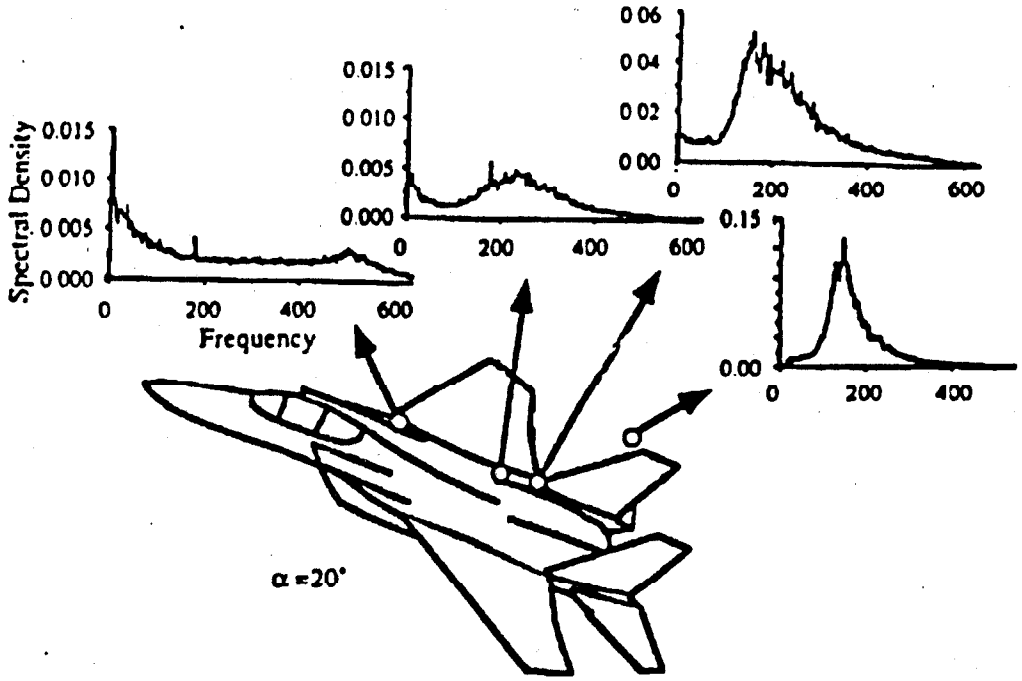

Figure 1 Hot-film velocity spectra measured above a 1/32-scale F-15 model at 33 m/s (ref. 6).

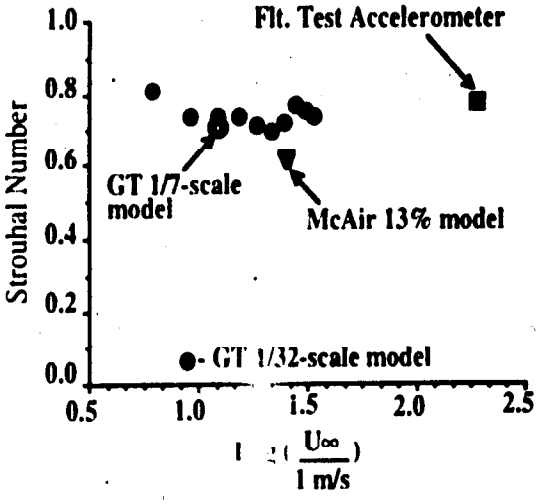

Figure 2 Strouhal number of velocity fluctuations based on m.a.c. over F-15 scale models and flight test data, α= 20 deg. (ref. 6).

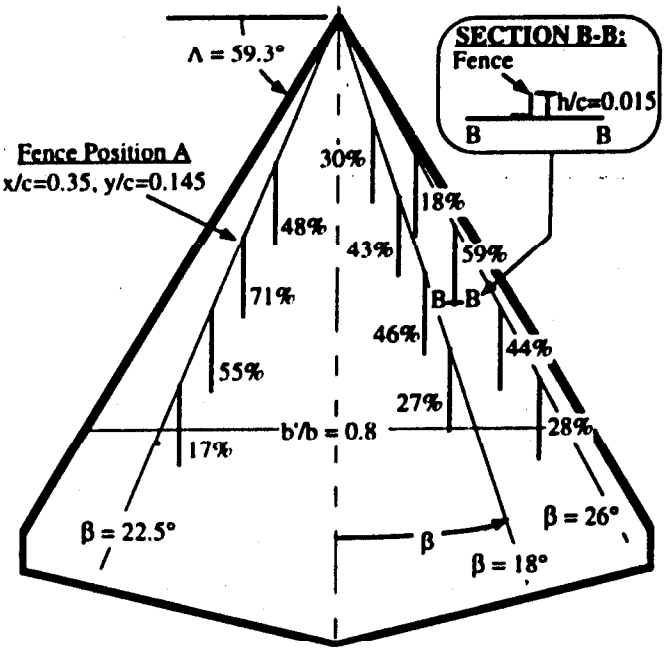

Figure 3 59.3°-Delta wing showing fence placement and percent reductions in spectral peak intensity: α= 25°, V_∞= 12.2 m/s (Ref. 9).

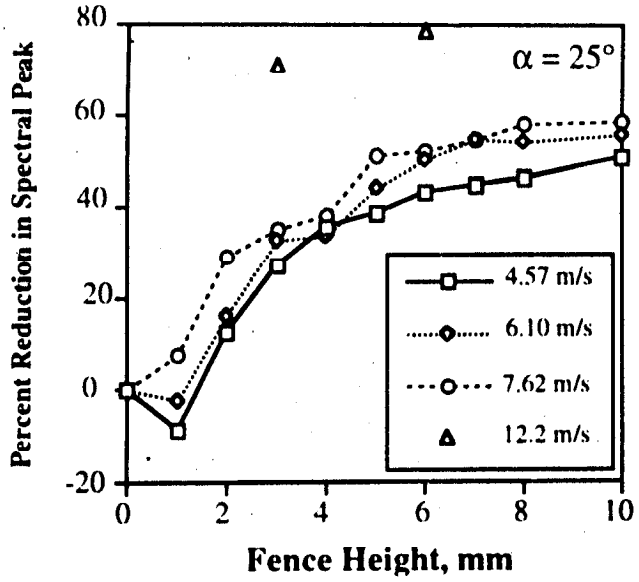

Figure 4 Effect of fence height on spectral peak intensity for 59.3°delta wing: fence position A (Ref. 9).

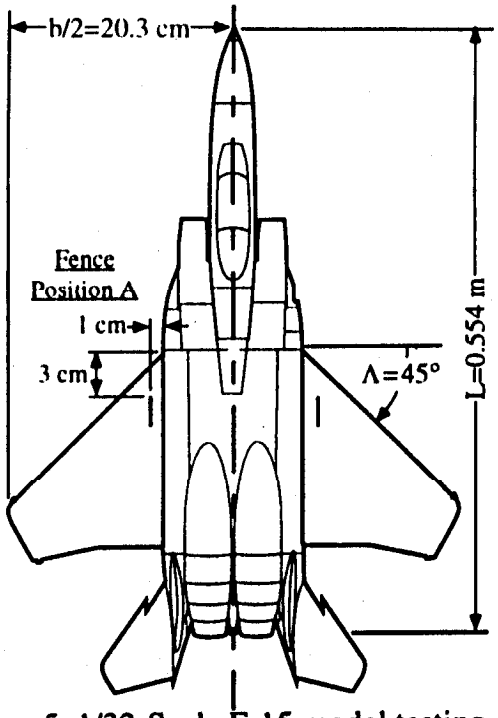

Figure 5 1/32-Scale F-15 model testing fences for reduction of tail buffet.

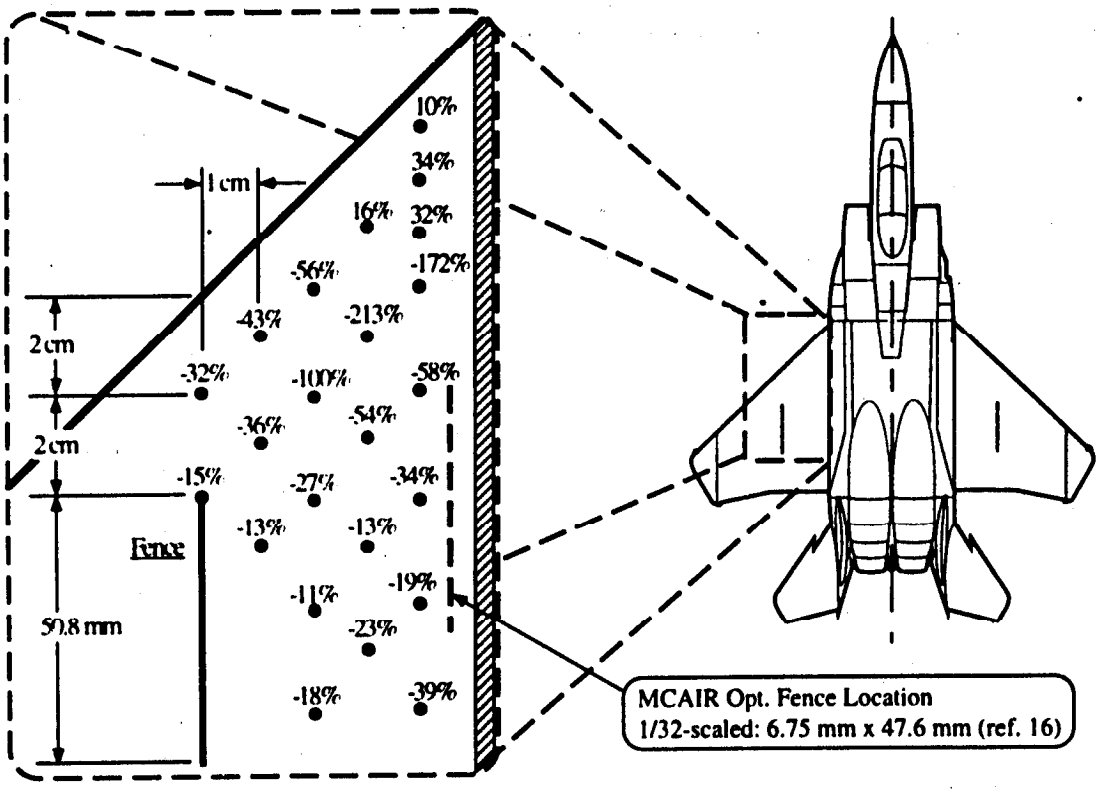

Figure 6 Percent reduction of spectral peak intensity with 3.5mm x 50.8mm fence placed at various locations on the F-15 wing surface: α=21.5° and V_∞=4.57 m/s.

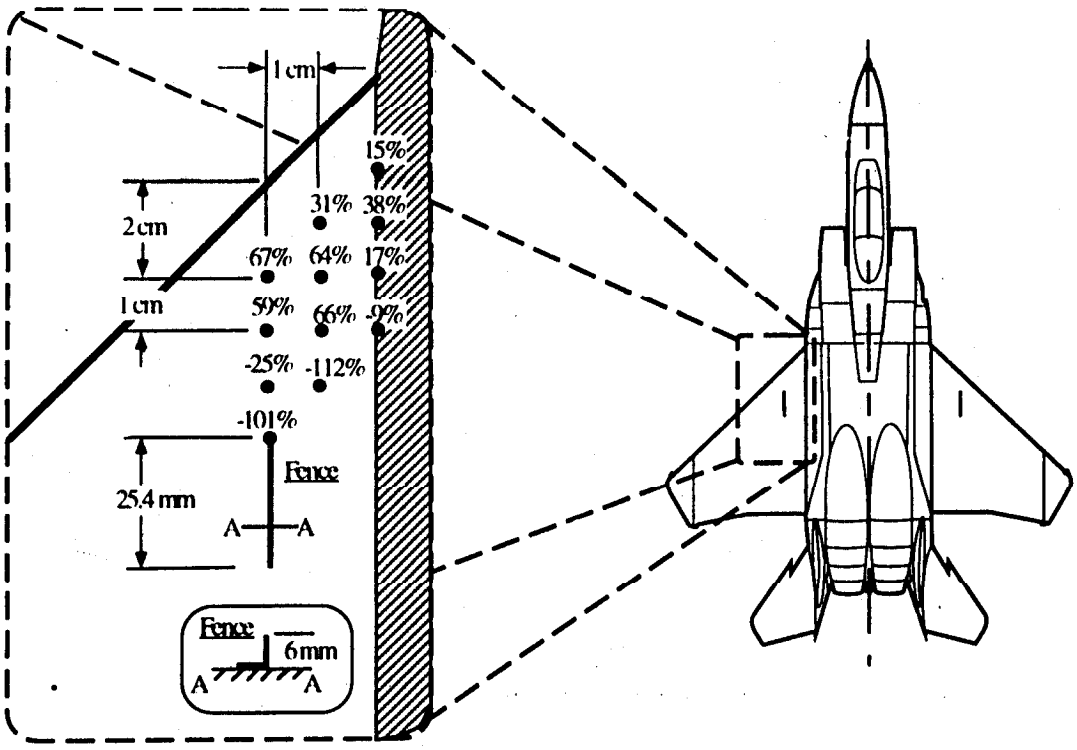

Figure 7 Percent reduction of spectral peak intensity with 6 mm x 25.4 mm fence placed at various locations on the F-15 wing surface: α=21.5° and V_∞=4.57 m/s.

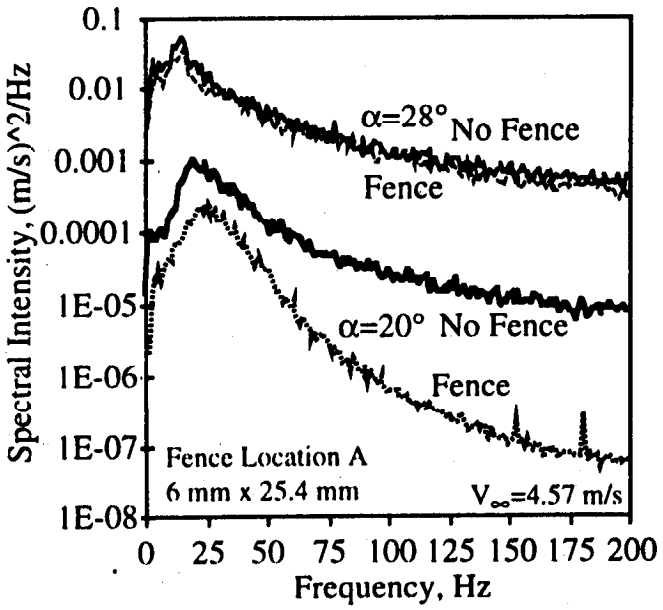

Figure 8 F-15 spectra for cases with- and without-fences at fence location A: α = 20° and α =28°.

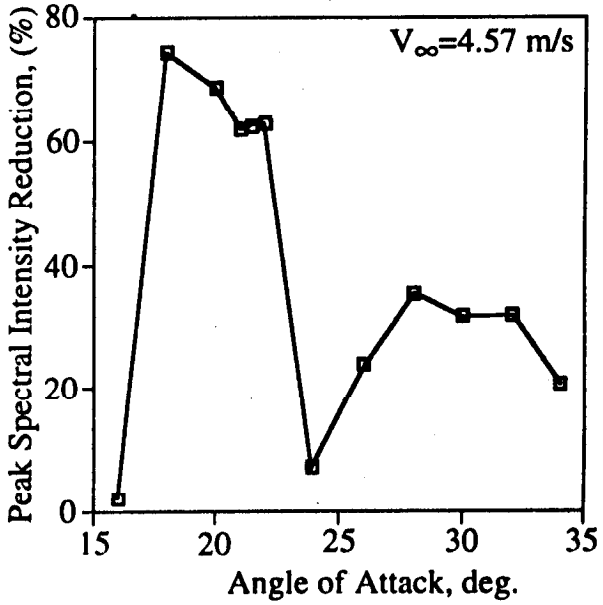

Figure 9 Percent spectral peak reductions as a function of angle of attack with 6 mm x 25.4 mm fences at location A.

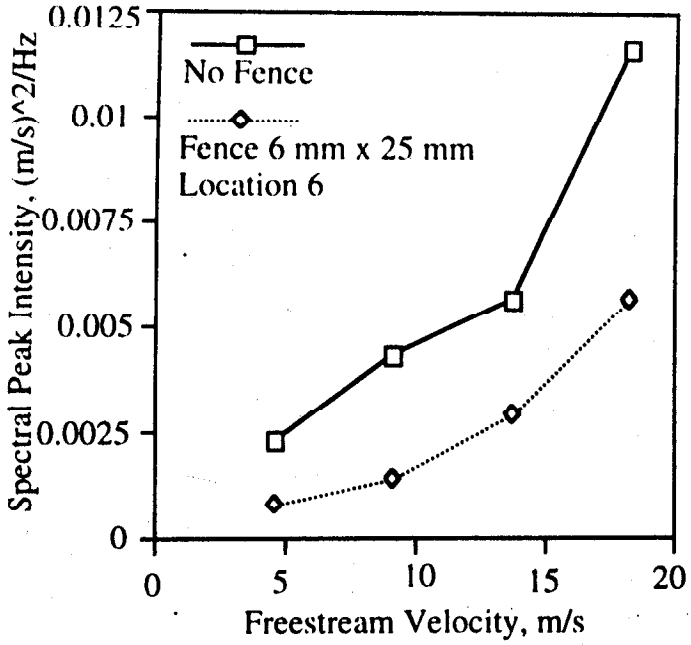

Figure 10 Spectral peak intensity variation with freestream speed for with- and without-fence cases at 21.5° angle of attack .

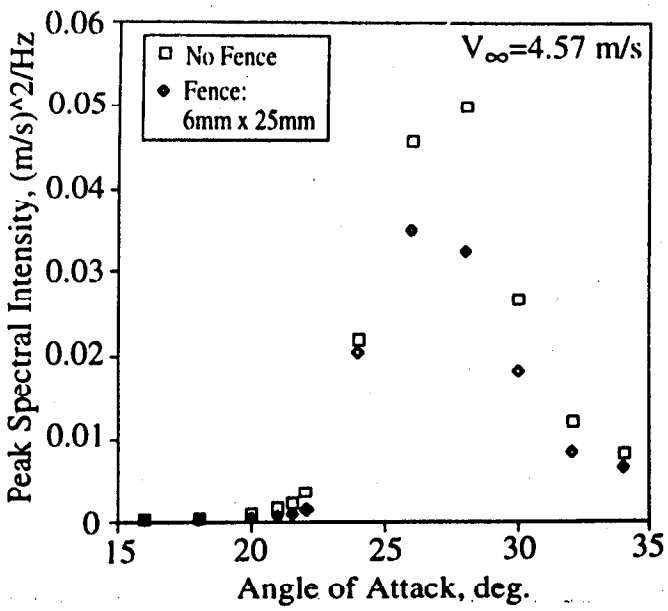

Figure 11 Magnitude spectral peak intensity as a function of angle of attack for F-15 model with and without fences at location A.

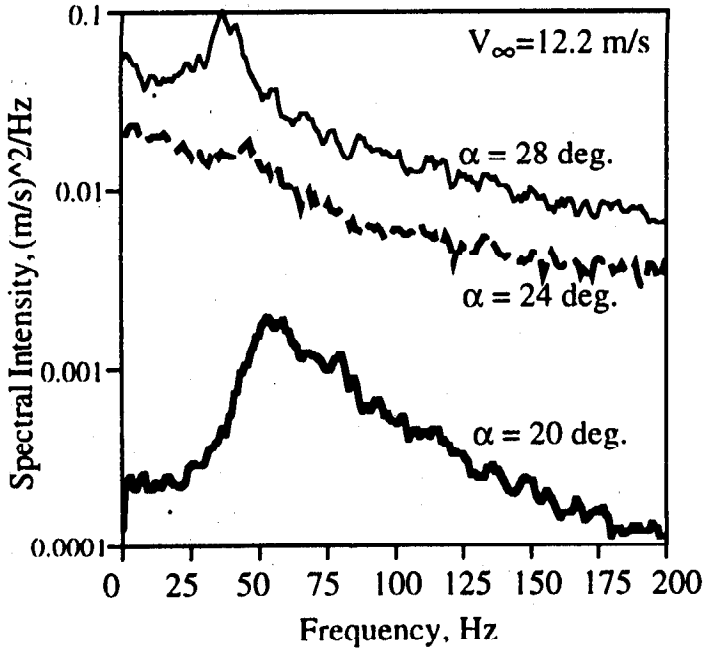

Figure 12 F-15 spectra at top of vertical tail for different angles of attack and constant velocity.

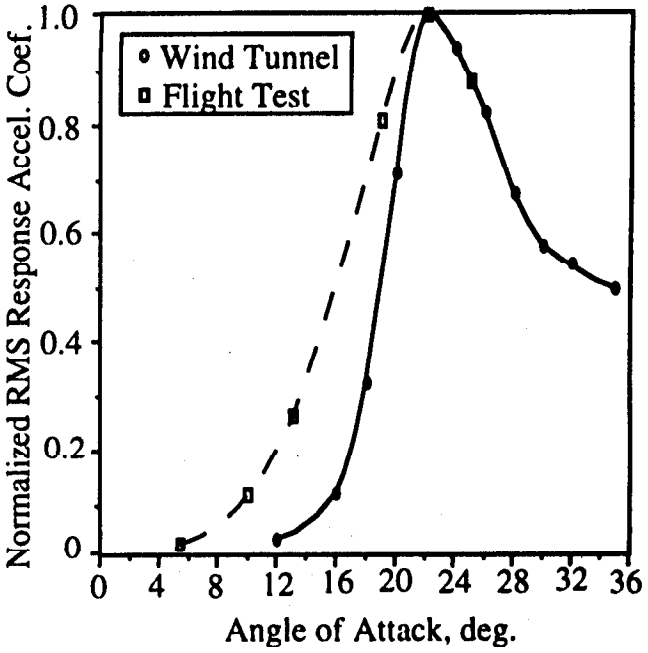

Figure 13 Comparison of normalized vertical tail aft pod responses in flight & wind tunnel tests (Colvin, et. al., MDC A6114, ref. 14).